Journal of Hazardous Materials 176 (2010) 569–574

Contents lists available at ScienceDirect

Journal of Hazardous Materials

journal homepage: www.elsevier.com/locate/jhazmat

Degradation of 4-nitrophenol (4-NP) using Fe–TiO_2 as a heterogeneous photo-Fenton catalyst

Binxia Zhao[a,*], Giuseppe Mele[b,**], Iolanda Pio[b], Jun Li[c], Leonardo Palmisano[d], Giuseppe Vasapollo[b]

[a] College of Chemical Engineering, Northwest University, 229 Taibai North Road, Xi'an, Shaanxi 710069, China
[b] Dipartimento di Ingegneria dell'Innovazione, Università del Salento, Via Arnesano, 73100 Lecce, Italy
[c] Shaanxi Key Laboratory of Physico-Inorganic Chemistry, Department of Chemistry, Northwest University, Xi'an, Shaanxi 710069, China
[d] "Schiavello-Grillone" Photocatalysis Group Dipartimento di Ingegneria Chimica dei Processi e dei Materiali, Università di Palermo, Viale delle Scienze, 90128 Palermo, Italy

ARTICLE INFO

Article history:
Received 17 June 2009
Received in revised form 6 November 2009
Accepted 10 November 2009
Available online 18 November 2009

Keywords:
Heterogeneous photocatalysis
4-Nitrophenol
Fe–TiO_2 photocatalysts

ABSTRACT

Photocatalytic degradation of 4-nitrophenol was investigated using Fe-doped (1, 3, 5 and 8 wt.% Fe) TiO_2 catalysts under UV light irradiation in aqueous dispersions in the presence of H_2O_2. Photocatalysts with the lowest Fe content (1%) showed a considerably better behavior with respect to the unloaded TiO_2 and the catalysts with higher Fe contents. Photocatalytic degradation was studied under different conditions such as amounts of 1% Fe–TiO_2 catalyst, H_2O_2 dose and initial pH of 4-NP solution. The results indicated that about 67.53% total organic carbon of a solution containing 20 mg L^{-1} 4-NP was removed at pH 6.17 by using 4.9 mM of H_2O_2 and 0.4 g L^{-1} of the catalyst in a 2-L batch photo-reactor, the complete degradation of 4-NP occurring after 60 min. It was also observed that catalytic behavior could be reproduced in consecutive experiments without a considerable decrease of the UV/Fe–TiO_2/H_2O_2 process efficiency.

1. Introduction

4-Nitrophenol (4-NP) is a toxic and bio-refractory pollutant which can cause considerable damage to the ecosystem and human health. It can damage the central nervous system, liver, kidney and blood of humans and animals. 4-NP and its derivatives are used in the production of pesticides, and as insecticides and herbicides [1]. Nitroaromatics are used in the production of explosives, and 4-NP is used in the production of many synthetic dyes [2]. Therefore, 4-NP and its derivatives are common pollutants in many natural water and industrial wastewater.

The conventional methods in industrial wastewater treatment are biological oxidation and physico-chemical processes (e.g. activated carbon adsorption, nano-filtration, coagulation–flocculation). Biological process results not sufficiently efficient since 4-NP is hardly removable due to its high stability and solubility in water. Physico-chemical processes have the main disadvantage that they are not destructive and they only transfer the contamination from one phase to another; hence, secondary wastes are produced and further treatments are necessary [3,4].

During the past two decades, advanced oxidation processes (AOPs) have been shown to be potentially advantageous and useful in the treatment of wastewater pollutants. Highly reactive and non-selective hydroxyl radicals that have the ability to oxidize most of the toxic and hazardous organic species in industrial effluents [5] are produced by AOPs in sufficient quantities. The UV/TiO_2/H_2O_2 process, for instance, has been applied successfully to mineralize organic contaminants transforming them into inorganic species or converting them into organic species readily biodegradable [6,7]. Heterogeneous photocatalysis by TiO_2 is gaining more importance in the last years, due to the fact that the used photocatalyst (often TiO_2 in the anatase form [8]) is inexpensive, nontoxic, abundantly available and (photo)stable. However, some limitations to the photocatalytic activity are the charge carrier recombination occurring within nanoseconds [9], the band edge absorption threshold less than 400 nm (wide band gap: 3.2 eV) and the low photon utilization efficiency [10]. Hence, the recent research is focused on the development of modified semiconductor photocatalysts to increase the efficiency of AOPs [11–14]. Also, it is experimentally found that the presence of iron in Fe–TiO_2 catalysts enhances the photocatalytic activity of TiO_2 by acting both as hole and electron traps [10].

A few researchers have reported the degradation of 4-NP by AOPs, including O_3, Fenton reagent, photo-Fenton and electro-Fenton methods, UV/H_2O_2, UV/TiO_2/H_2O_2, UV/TiO_2 and ultrasonic irradiation [15–21], etc. However, to our knowledge, there has been little research investigating the degradation of 4-NP by the UV/Fe–TiO_2/H_2O_2 process.

* Corresponding author. Tel.: +86 29 88302632; fax: +86 29 88373052.
** Corresponding author. Tel.: +39 0832 297281; fax: +39 0832 297733.
E-mail addresses: zxlbx@china.com (B. Zhao), giuseppe.mele@unisalento.it (G. Mele).

0304-3894/$ – see front matter © 2009 Elsevier B.V. All rights reserved.
doi:10.1016/j.jhazmat.2009.11.066

So that, aim of this study was to investigate the applicability of Fe-doped TiO_2 as heterogeneous photo-Fenton catalyst for the minimization of the organic content in model wastewater containing 4-NP. The effect of Fe content in Fe–TiO_2 (1, 3, 5 and 8 wt.% Fe) on the photocatalytic activity was investigated and the Fe content was optimized. The influence of various parameters such as amount of Fe–TiO_2 catalyst, H_2O_2 dose and initial pH of 4-NP solution on the efficiency of the process was assessed. The efficiency of the system was evaluated by following the concentration of 4-NP and total organic carbon (TOC) under irradiation; the (photo)stability of Fe–TiO_2 catalyst was checked by carrying out consecutive experiments.

2. Materials and methods

2.1. Reagents

4-Nitrophenol was obtained from Aldrich and used without further purification. The hydrogen peroxide solution (30%) and $Fe(NO_3)_3$•$9H_2O$ were purchased from Aldrich. Solutions were prepared by dissolving the required quantity of 4-NP in water obtained by a New Human Power I water purification system.

2.2. Preparation of Fe–TiO_2

TiO_2 (anatase phase, specific surface area 8 m^2/g), provided by Tioxide Huntsman, was dried, crushed and sieved to obtain particles with a diameter smaller than 0.1 mm. Loading was performed by impregnating TiO_2 with aqueous solutions of $Fe(NO_3)_3 \cdot 9H_2O$ by an incipient wetness impregnation method as described in the following. The mixture (TiO_2 and $Fe(NO_3)_3$) was stirred at room temperature during 24 h. Subsequently the catalysts were dried overnight at 393 K by using an oil bath. Finally, the catalysts were calcined for 5 h in a furnace whose temperature was increased from room temperature to 350 °C. After calcinations, the catalysts (1, 3, 5 and 8%) Fe–TiO_2 were stored in a desiccator. The percentage of metal was calculated as [(weight of metal)/(weight of TiO_2)] × 100.

2.3. Characterization of Fe–TiO_2

X-ray diffraction patterns of the Fe–TiO_2 photocatalysts, performed by using a powder diffractometer (Model: Ultima$^+$ Rigaku) equipped with a Cu Kα radiation, were used to determine the identity of any phase present and their crystallite size. The accelerating voltage and current used were 40 kV and 26 mA, respectively. The 2θ ranged from 20° to 80°. The average crystallite size of catalysts was obtained by means of the Scherrer equation [$D = 0.89\lambda/\beta\cos\theta$, where D is the crystallite size (nm), λ is the wavelength (nm), β is the corrected full width at half maximum (radian) and θ is the Bragg angle (radian)]. The morphology of the Fe–TiO_2 photocatalysts was studied by using a scanning electron microscopy (SEM) Zeiss Evo 40.

2.4. Photo-reactor and procedures

The photoreactivity experiments were carried out by using a photo-reactor (ECO 12 H) kindly supplied by Novus srl-Brindisi (Italy). An UV lamp, with a monochromatic radiation at 340 nm and radiant flux of 100 μW cm^{-2}, was housed in a double-walled quartz sleeve inside the glass reactor. The reactor was placed in a box made of stainless steel to prevent loss of UV light. 4-NP solution in a glass vessel (2.5 dm^3) was pumped into the photo-reactor after oxygenation by bubbling air. The experimental setup is sketched in Fig. 1.

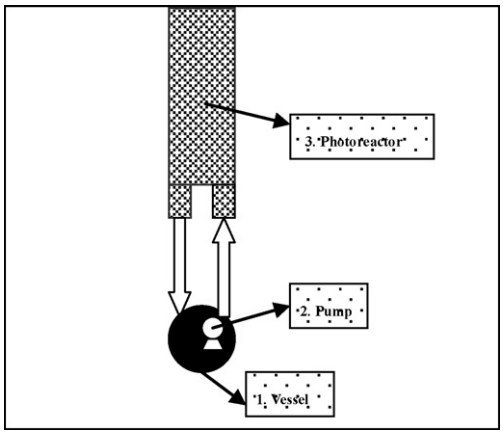

Fig. 1. Setup of the photocatalytic system. 1. Batch photo-reactor containing the solution of 4-NP/water and the suspended photocatalyst. 2. Pump for the recirculation of the solution/photocatalyst suspension. 3. Photo-reactor for the UV irradiation which consists of a lamp irradiating two fluoropolymer tubes having UV transparency.

For irradiation experiment, 2 dm^3 of 4-NP suspension were fed into the glass vessel. The suspension was stirred magnetically for 1 h in the dark. The pH of the reaction mixture was the natural pH of dissolved 4-NP (about 6.17) except for experiments studying the influence of pH for which the pH was adjusted by using H_2SO_4 or NaOH solutions. A defined content of H_2O_2 was added to the mixture and the lamp was switched on to initiate the reaction. At fixed intervals of time, 5 mL of sample were withdrawn and filtered by using 0.45 μm nylon filters to remove catalyst particles before analyses of the solution.

2.5. Analysis

The degradation of 4-NP was measured with UV–vis spectrophotometer (Cary 100 Scan, VARIAN) at 316 nm. Different calibration curves calculated at different pH values of 3, 4, 5, 6 and 8 depending on the pH value measured when the sampling were used. The extent of mineralization of the 4-NP was determined on the basis of total organic carbon measurement using a TOC analyzer (IL550 TOC-TN, HACH-LANGE). Measurements of Fe^{3+} in solution were measured according with the UNI-EN-ISO 11885 method using an ICP spectrometer THERMO SCIENTIFIC iCAP 6000 SERIES.

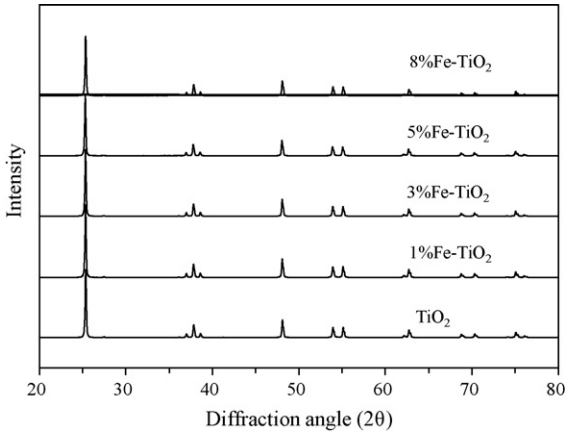

Fig. 2. XRD patterns of Fe-doped and undoped mixed crystal TiO_2 powders.

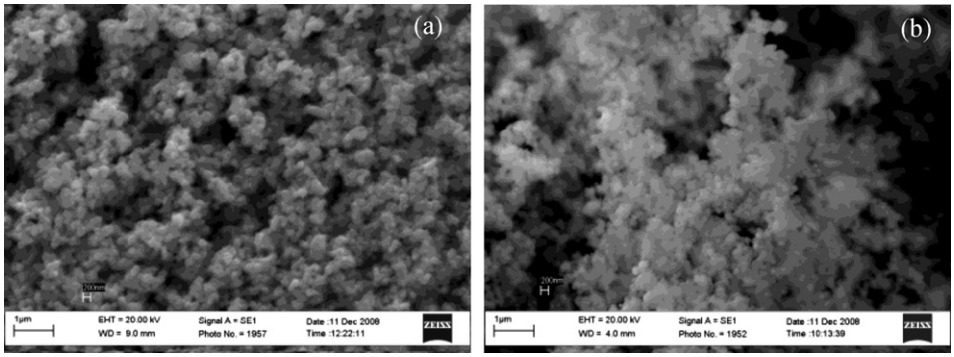

Fig. 3. SEM images of (a) TiO_2 and (b) 1% Fe–TiO_2 calcined at 350 °C for 5 h.

3. Results and discussion

3.1. Catalyst characteristics

The XRD diffractogram patterns of the samples (0, 1, 3, 5 and 8%) Fe–TiO_2 calcined at 350 °C for 5 h are shown in Fig. 2. The XRD patterns of Fe-doped TiO_2 samples almost coincide with that of the bare TiO_2 sample. It can be noticed that the presence of anatase TiO_2 type structure in all Fe loaded TiO_2 catalysts, without significant difference with the bare TiO_2 sample. This finding can be explained by considering that the Fe^{3+} content in the Fe–TiO_2 samples is below the detection limit or that amorphous iron oxides species are very dispersed onto the surface of TiO_2 particles. Another explanation is that all Fe^{3+} ions might substitute Ti^{4+} ions and insert into the crystal lattice of TiO_2 (at least only into the very top layers of the crystallites, due to the relatively low temperature of heating at which the diffusion extent of the ions cannot be very significant) because the radius of Fe^{3+} (0.69 Å) is similar to that of Ti^{4+} (0.745 Å) [22–24]. The crystallite size of the catalysts was calculated from the line broadening. The diameters are 50.5, 45.9, 50.3, 50.0 and 49.7 nm for samples with 0, 1, 3, 5 and 8 wt.% iron content, respectively. Analysis of SEM picture (Fig. 3) shows that 1% Fe-doped TiO_2 catalyst contains a higher number of irregular shaped particles. Moreover, the sizes of the Fe-doped particles, consisting of aggregates of tiny crystals, are smaller compared to that of the bare TiO_2 sample, in agreement with the XRD results. The presence of Fe^{3+} ions seems to hamper the growth of TiO_2 particles.

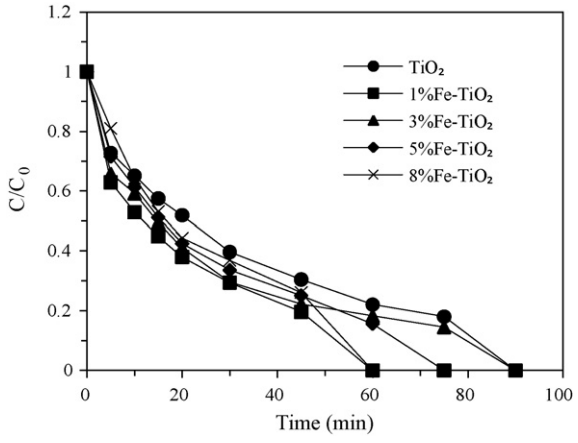

Fig. 4. Effect of Fe content in Fe–TiO_2 on degradation efficiency of the process ([4-NP]$_0$ = 20 mg L^{-1}, pH = 6.17, [H_2O_2]$_0$ = 4.9 mM, catalyst amount = 0.4 g L^{-1}).

3.2. Effect of Fe content in Fe–TiO_2

Compared to pure TiO_2, the Fe–TiO_2 catalysts exhibited a significant increase in 4-NP photodegradation efficiency as shown in Fig. 4 where C_0 and C are the concentrations of 4-NP before and after starting the light irradiation, respectively. It can be observed that the presence of iron species influences the photocatalytic activity. At the beginning, the photocatalytic activity of the catalysts decreased with the increase of Fe^{3+} loaded onto TiO_2, while after 45 min it increased by further increasing the Fe^{3+} content, except for the 1% Fe–TiO_2 sample. This finding can be explained by taking into account the occurrence of a high iron ions leaching into solution. All of the doped samples showed to be more photoactive than bare TiO_2 and the optimal amount of Fe^{3+} is 1%. 67.53% TOC of a solution containing 20 mg L^{-1} 4-NP, for instance, was removed after 60 min of irradiation by using the 1% Fe–TiO_2 sample. The beneficial effect of the presence of Fe^{3+} species on the photocatalytic activity could be due to the role of Fe^{3+} species acting as h^+/e^- traps, thus hindering the recombination rate and enhancing the photocatalytic activity. The detailed reaction steps are as follows [25,26]:

$$Fe^{3+} + e^- \rightarrow Fe^{2+} \quad (1)$$

$$Fe^{2+} + O_{2(ads)} \rightarrow Fe^{3+} + O_2^{\bullet -} \quad (2)$$

$$Fe^{2+} + Ti^{4+} \rightarrow Fe^{3+} + Ti^{3+} \quad (3)$$

$$Fe^{3+} + h_{vb}{}^+ \rightarrow Fe^{4+} \quad (4)$$

$$Fe^{4+} + OH^- \rightarrow Fe^{3+} + HO^{\bullet} \quad (5)$$

It should be noted, however, that Fe^{3+} ions can also act as recombination centers for the h^+/e^- pairs when their concentration is high, according to the following reactions [25]:

$$Fe^{3+} + e^- \rightarrow Fe^{2+} \quad (6)$$

$$Fe^{2+} + h_{vb}{}^+ \rightarrow Fe^{3+} \quad (7)$$

Consequently the presence of iron species, especially at low levels, inhibits the recombination rate of h^+/e^- pair and enhances the photocatalytic activity. When the amount of iron ions is increased, they become recombination centers resulting in lowered photocatalytic activity. It has been also proved that the excess of deposited iron on TiO_2 can form $Fe(OH)^{2+}$ species, with a greater absorption of the incident light in the range 290–400 nm with respect to bare TiO_2. This competition in photon absorption subtracts photon to TiO_2 and can be considered responsible (along with other factors as above reported) for the decrease of the photocatalytic activity of the Fe–TiO_2 samples [27].

When other published investigations [25,26] are scrutinized it can be noticed that the effect of iron species content in Fe–TiO_2 on the photocatalytic activity is not obvious. The differences in photocatalytic activity are likely due to differences in BET-surface areas.

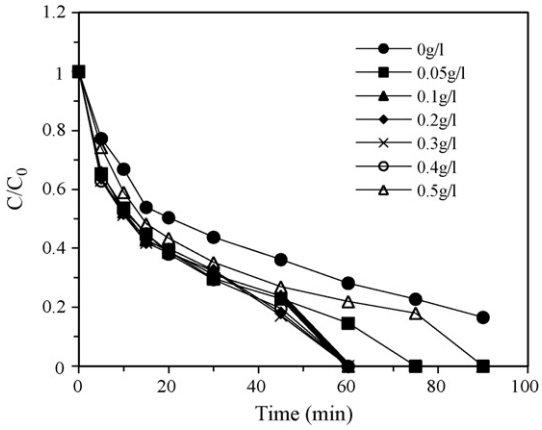

Fig. 5. Effect of photocatalyst loading on degradation efficiency of the process ([4-NP]$_0$ = 20 mg L^{-1}, pH = 6.17, [H_2O_2]$_0$ = 4.9 mM, photocatalyst: 1% Fe–TiO_2).

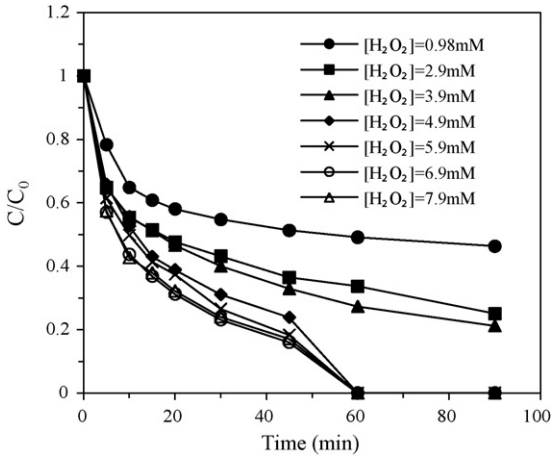

Fig. 6. Effect of initial concentration of H_2O_2 on degradation efficiency of the process ([4-NP]$_0$ = 20 mg L^{-1}, pH = 6.17, catalyst amount [1% Fe/TiO_2] = 0.1 g L^{-1}).

In fact, the specific surface areas of the samples used in refs. [25,26] (51–76.3 m^2/g [25] and 65.1–85.6 m^2/g [26]) are much larger than that of ours (only about 8 m^2/g). Moreover other morphological and physico-chemical parameters, as for instance impurities, lattice mismatches and density of surface hydroxyl groups, can affect not only the adsorption extent of the starting molecule and/or the intermediates, but also the recombination rate and thus the lifetime of the photoproduced electron–hole pairs. Further investigation will be aimed to characterize more deeply the surface of the photocatalysts in order to obtain insights on this point.

3.3. Effect of catalyst loading

To determine the effect of the catalyst loading, a series of experiments was carried out by varying the amount of catalyst from 0.1 to 0.5 g L^{-1}. The influence of photocatalyst loading on degradation efficiency versus time is reported in Fig. 5. It can be observed that the efficiency of the heterogeneous photo-Fenton process increased by increasing the photocatalyst amount up to 0.1 g L^{-1}, and the removal efficiency was nearly constant from 0.1 g L^{-1} to 0.4 g L^{-1}, then decreased above 0.4 g L^{-1}. A very small amount of photocatalyst showed to be sufficient for the occurrence of heterogeneous photo-Fenton degradation of 2 L of 20 mg L^{-1} of 4-NP. The enhancement of the removal efficiency was due to the increase of active sites available for the photo-Fenton catalytic reaction as the loading of Fe–TiO_2 increased up to the optimum value; higher values, instead, gave rise to more important phenomena of light screening and scattering, decreasing the penetration depth of the light into the suspension [28–30]. Consequently, the overall number of photons reaching the photocatalyst surface decreased as well as the number of photo generated active sites producing •OH radicals by decomposition of H_2O_2 molecules [31].

3.4. Effect of the initial concentration of H_2O_2

The heterogeneous photo-Fenton degradation of 4-NP has been studied at different H_2O_2 concentrations and the results are summarized in Fig. 6. The removal efficiency of 4-NP increased with increasing the concentration up to 5.9 mM. For higher concentrations no significant additional improvement was observed. The beneficial effect can be attributed to the increase of the concentration of hydroxyl radicals generated by photolytic peroxidation (UV and H_2O_2), as shown in the following equations (see Eqs. (8) and (11)).

$$H_2O_2 + h\nu \rightarrow 2^{\bullet}OH \quad (8)$$

$$H_2O_2 + e^-_{CB} \rightarrow {}^{\bullet}OH + OH^- \quad (9)$$

$$H_2O_2 + Fe^{2+} \rightarrow Fe^{3+} + {}^{\bullet}OH + OH^- \quad (10)$$

$$RH + {}^{\bullet}OH \rightarrow H_2O + R^{\bullet} \rightarrow \text{further oxidation} \quad (11)$$

At the highest concentrations, the reaction between H_2O_2 and strong oxidant •OH radicals and/or h_{vb}^+ became more relevant (see Eqs. (12) and (13)) and as a consequence no subsequent improvement on the heterogeneous photo-Fenton oxidation rate can be noticed because the produced HO_2 radicals are less reactive than both •OH radicals and h^+_{vb} [32].

$$H_2O_2 + 2h_{vb}^+ \rightarrow O_2 + 2H^+ \quad (12)$$

$$H_2O_2 + {}^{\bullet}OH \rightarrow HO_2{}^{\bullet} + H_2O \quad (13)$$

3.5. Effect of the initial pH

pH plays an important role in photocatalytic abatement of various pollutants [33,34]. The influence of pH of 4-NP solution on the UV/Fe–TiO_2/H_2O_2 process efficiency was studied by using six various initial pH values (3.56, 3.89, 4.28, 5.15, 6.43 and 8.23) without changing or checking them throughout all the process. In Fig. 7, the obtained results for 4-NP degradation as a function of the initial pH of the solution at various reaction times are displayed. The degradation efficiency decreased rapidly with increasing the pH value. This can be explained by considering that (i) under strong alkaline condition, CO_2 produced during the 4-NP degradation was converted

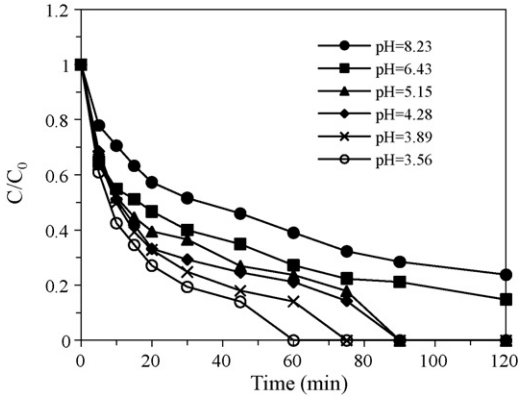

Fig. 7. Effect of initial pH on degradation efficiency of the process ([4-NP]$_0$ = 20 mg L^{-1}, [H_2O_2]$_0$ = 3.9 mM, catalyst amount [1% Fe/TiO_2] = 0.1 g L^{-1}).

Table 1
Changes in pH of the 4-NP solution during the process[a].

Degradation time (min)	pH				
0	6.43	5.15	4.28	3.89	3.56
10	6.73	6.6	4.75	4.58	4.18
30	6.25	5.66	4.43	4.39	4.13
60	5.97	5.58	4.65	4.53	4.6
90	6.35	5.86	5.43	5.23	5.3
120	6.62	6.23	5.97	5.89	5.89

[a] $[4\text{-NP}]_0 = 20\ mg\ L^{-1}$, $[H_2O_2]_0 = 3.9\ mM$, catalyst amount $[1\%\ Fe/TiO_2] = 0.1\ g\ l^{-L}$.

to CO_3^{2-} and HCO_3^-, both of which are able to react with hydroxyl radical by the following reactions [35]:

$$CO_3^{2-} + {}^{\bullet}OH \rightarrow CO_3^{\bullet-} + {}^{-}OH \quad k = 3.9 \times 10^8\ M^{-1}s^{-1} \tag{14}$$

$$HCO_3^- + {}^{\bullet}OH \rightarrow CO_3^{\bullet-} + H_2O \quad k = 8.5 \times 10^6\ M^{-1}s^{-1} \tag{15}$$

The inorganic radical anions show a much lower reactivity than •OH and they do not take part in the 4-NP mineralization. Moreover a drastic competition between 4-NP and the anions with respect to •OH can be envisaged; (ii) alkaline conditions favoured the dissociation of hydrogen peroxide to form HO_2^- as shown in the Eq. (16):

$$H_2O_2 \rightarrow HO_2^- + H^+ \tag{16}$$

HO_2^- reacts with a non-dissociated molecule of H_2O_2 according to Eq. (17) which leads to oxygen and water, instead of hydroxyl radicals under UV radiation. Therefore, the instantaneous concentration of •OH is lower than that expected.

$$HO_2^- + H_2O_2 \rightarrow H_2O + O_2 + OH^- \tag{17}$$

This effect is more important when the pH of the solution is high. HO_2^- ions, in fact, have a higher reactivity than hydrogen peroxide with hydroxyl radicals, resulting in a decrease in their number [36].

$$^{\bullet}OH + HO_2^- \rightarrow H_2O + O_2^{-\bullet} \quad k = 7.5 \times 10^9\ M^{-1}s^{-1} \tag{18}$$

$$^{\bullet}OH + H_2O_2 \rightarrow H_2O + HO_2^{\bullet} \quad k = 2.7 \times 10^7\ M^{-1}s^{-1} \tag{19}$$

It can be observed in Table 1 the increase of pH during the first 10 min of irradiation time, due to the increase of the concentration of OH^- generated by decomposition of hydrogen peroxide (see Eqs. (9) and (17)), and a subsequent drop from 10 to 30 min, due to the formation of acidic species some of which can be produced by the oxidative demolition of organics deriving from the degradation of 4-NP. The increase of pH is also observed after ca. 40 min to reach final values always higher than the initial one in a narrow range close to 6 pH units.

3.6. Stability of Fe–TiO_2

As well known, the photostability of the catalytic systems is one of the important factors for practical application. For this reason, recycling experiment where carried out using 1% Fe–TiO_2 photocatalyst in order to determine its stability. In particular, the 1% Fe–TiO_2 of the photocatalysts was recovered by filtration from the solution after treatment, washed with ultra-pure water, dried at 110 °C overnight and then reused under the same reaction conditions ($[4\text{-NP}]_0 = 20\ mg\ L^{-1}$, pH = 6.17, $[H_2O_2]_0 = 4.9\ mM$, catalyst amount $[1\%\ Fe/TiO_2] = 0.4\ g\ L^{-1}$). After three runs, the photocatalyst was calcined at 350 °C for 5 h and then tested again. 67.53%, 64.17%, 62.32% and 66.26% TOC of 4-NP solution were removed by multi-run consecutive experiments, respectively. The results indicate that the photoactivity of 1% Fe–TiO_2 was virtually unchanged after four consecutive experiments.

Moreover, the catalytic behavior could be reproduced after that the photocatalysts were subjected to calcinations, due to decomposition of the adsorbed intermediates and the restoration of the adsorption sites. This finding indicates the absence of significant deactivation.

Finally, very low amounts of Fe^{3+} ions dissolved in solution (1–8 ppb) were detected by ICP measurement carried out for selected experiments. These amounts can be considered negligible compared with the total amount of Fe^{3+} deposited onto the TiO_2 surface (1–40 ppm). For this reason, although a possible contribution of the homogeneous Fenton reaction occurring in the process can be not excluded; however, this contribution can be considered negligible compared with the contribution of the heterogeneous photo-Fenton process.

4. Conclusions

Fe–TiO_2 can efficiently catalyze the degradation of 4-NP under UV light irradiation in the presence of H_2O_2. The photocatalyst 1% Fe–TiO_2 was found to be more efficient than bare TiO_2. Catalyst and H_2O_2 concentration, initial pH of 4-NP solution are important variables on the process efficiency. The optimum concentrations of catalyst and H_2O_2 for enhanced efficiency are $0.1\ g\ L^{-1}$ and 4.9 mM, respectively. The degradation of 4-NP by the UV/Fe–TiO_2/H_2O_2/process is more favorable in acidic than in alkaline pH. Under these optimum conditions, this process can be effectively applied for the treatment of wastewater containing 4-NP. It is also observed that catalytic behavior could be reproduced in consecutive experiments without a considerable drop in the process efficiency. Moreover, the releasing of Fe^{3+} in solution was demonstrated be negligible occurring the heterogeneous photo-Fenton process.

Acknowledgement

We thank Huntsman Tioxide for giving us the bare TiO_2 sample and NOVUS srl for giving us the photo-reactor used in this work.

References

[1] M.S. Dieckmann, K.A. Gray, A comparison of the degradation of 4-nitrophenol via direct and sensitized photocatalysis in TiO_2 slurries, Water Res. 30 (1996) 1169–1183.
[2] N. Takahashi, T. Nakai, Y. Satoh, Y. Katoh, Variation of biodegradability of nitrogenous organic compounds by ozonation, Water Res. 28 (1994) 1563–1570.
[3] Y.E. Benkli, M.F. Can, M. Turan, M.S. Celik, Modification of organo-zeolite surface for the removal of reactive azo dyes in fixed-bed reactors, Water Res. 39 (2005) 487–493.
[4] N. Daneshvar, H. Ashassi Sorkhabi, M.B. Kasiri, Decolorization of dye solution containing Acid Red 14 by electrocoagulation with a comparative investigation of different electrode connections, J. Hazard. Mater. 112 (2004) 55–62.
[5] A. Aleboyeh, H. Aleboyeh, Y. Moussa, "Critical" effect of hydrogen peroxide in photochemical oxidative decolorization of dyes: Acid Orange 8, Acid Blue 74 and Methyl Orange, Dyes Pigments 57 (2003) 67–75.
[6] M. Saquib, M. Abu Tariq, M.M. Haque, M. Muneer, Photocatalytic degradation of disperse blue 1 using UV/TiO_2/H_2O_2 process, J. Environ. Manage. 88 (2008) 300–306.
[7] H. Seshadri, S. Chitra, K. Paramasivan, P.K. Sinha, Photocatalytic degradation of liquid waste containing EDTA, Desalination 232 (2008) 139–144.
[8] S.S. Hong, M.S. Lee, C.S. Ju, G.D. Lee, S.S. Park, K.T. Lim, Photocatalytic decomposition of p-nitrophenol over titanium dioxides prepared in water-in-carbon dioxide microemulsion, Catal. Today 93–95 (2004) 871–876.
[9] N. Serpone, D. Lawless, J. Disdier, J.M. Herrmann, Spectroscopic, photoconductivity, and photocatalytic studies of TiO_2 colloids: naked and with the lattice doped with Cr^{3+}, Fe^{3+}, and V^{5+} cations, Langmuir 10 (1994) 643–652.
[10] J.F. Zhu, W. Zheng, B. He, J.L. Zhang, M. Anpo, Characterization of Fe–TiO_2 photocatalysts synthesized by hydrothermal method and their photocatalytic reactivity for photodegradation of XRG dye diluted in water, J. Mol. Catal. A: Chem. 216 (2004) 35–43.
[11] A. Dobosz, A. Sobczynski, The influence of silver additives on titania photoactivity in the photooxidation of phenol, Water Res. 37 (2003) 1489–1496.
[12] J.C. Colmenars, M.A. Aramendía, A. Marinas, J.M. Marinas, F.J. Urbano, Synthesis, characterization and photocatalytic activity of different metal-doped titania systems, Appl. Catal. A: Gen. 306 (2006) 120–127.
[13] B. Tryba, A.W. Morawski, M. Inagaki, M. Toyoda, The kinetics of phenol decomposition under UV irradiation with and without H_2O_2 on TiO_2,

Fe–TiO_2 and Fe–C–TiO_2 photocatalysts, Appl. Catal. B: Environ. 63 (2006) 215–221.
[14] N. Sobana, K. Selvam, M. Swaminathan, Optimization of photocatalytic degradation conditions of Direct Red 23 using nano-Ag doped TiO_2, Sep. Purif. Technol. 62 (2008) 648–653.
[15] A. Kotronarou, G. Mills, M.R. Hoffmann, Ultrasonic irradiation of p-nitrophenol in aqueous solution, J. Phys. Chem. 95 (1991) 3630–3638.
[16] F.J. Beltrán, V. Gómez-Serrano, A. Durán, Degradation kinetics of p-nitrophenol ozonation in water, Water Res. 26 (1992) 9–17.
[17] E. Lipczynska-Kochany, Degradation of nitrobenzene and nitrophenols by means of advanced oxidation processes in a homogeneous phase: photolysis in the presence of hydrogen peroxide versus the Fenton reaction, Chemosphere 24 (1992) 1369–1380.
[18] D.W. Chen, A.K. Ray, Photodegradation kinetics of 4-nitrophenol in TiO_2 suspension, Water Res. 32 (1998) 3223–3234.
[19] M.A. Oturan, J. Peiroten, P. Chartrain, A.J. Acher, Complete destruction of p-nitrophenol in aqueous medium by electro-Fenton method, Environ. Sci. Technol. 34 (2000) 3474–3479.
[20] W.B. Zhang, X.M. Xiao, T.C. An, Z.G. Song, J.M. Fu, G.Y. Sheng, M.C. Cui, Kinetics, degradation pathway and reaction mechanism of advanced oxidation of 4-nitrophenol in water by a UV/H_2O_2 process, J. Chem. Technol. Biotechnol. 78 (2003) 788–794 (online).
[21] N. Daneshvar, M.A. Behnajady, Y. Zorriyeh Asghar, Photooxidative degradation of 4-nitrophenol (4-NP) in UV/H_2O_2 process: influence of operational parameters and reaction mechanism, J. Hazard. Mater. 139 (2007) 275–279.
[22] R.I. Bickley, J.S. Lees, R.J.D. Tilley, L. Palmisano, M. Schiavello, Characterisation of iron/titanium oxide photocatalysts. Part 1. Structural and magnetic studies, J. Chem. Soc., Faraday Trans. 88 (1992) 377–384.
[23] C.Y. Wang, C. Bottcher, D.W. Bahnemann, J.K. Dohrmann, A comparative study of nanometer sized Fe(III)-doped TiO_2 photocatalysts: synthesis, characterization and activity, J. Mater. Chem. 13 (2003) 2322–2329.
[24] M.H. Zhou, J.G. Yu, B. Cheng, Effects of Fe-doping on the photocatalytic activity of mesoporous TiO_2 powders prepared by an ultrasonic method, J. Hazard. Mater. 137 (2006) 1838–1847.
[25] Z. Ambrus, N. Balázs, T. Alapi, G. Wittmann, P. Sipos, A. Dombi, K. Mogyorósi, Synthesis, structure and photocatalytic properties of Fe(III)-doped TiO_2 prepared from $TiCl_3$, Appl. Catal. B: Environ. 81 (2008) 27–37.
[26] J. Yu, Q. Xiang, M. Zhao, Preparation, characterization and visible-light-driven photocatalytic activity of Fe-doped titania nanorods and first-principles study for electronic structures, Appl. Catal. B: Environ. 90 (2009) 595–602.
[27] X.H. Qi, Z.H. Wang, Y.Y. Zhuang, Y. Yu, J.L. Li, Study on the photocatalysis performance and degradation kinetics of X-3B over modified titanium dioxide, J. Hazard. Mater. 118 (2005) 219–225.
[28] A.B. Prevot, M. Vincenti, A. Bianciotto, E. Pramauro, Photocatalytic and photolytic transformation of chloramben in aqueous solutions, Appl. Catal. B: Environ. 22 (1999) 149–158.
[29] D. Robert, B. Dongui, J.V. Weber, Heterogeneous photocatalytic degradation of 3-nitroacetophenone in TiO_2 aqueous suspension, J. Photochem. Photobiol. A: Chem. 156 (2003) 195–200.
[30] N. Daneshvar, D. Salari, A.R. Khataee, Photocatalytic degradation of azo dye acid red 14 in water on ZnO as an alternative catalyst to TiO_2, J. Photochem. Photobiol. A: Chem. 162 (2004) 317–322.
[31] Y.M. Li, Y.Q. Lu, X.L. Zhu, Photo-Fenton discoloration of the azo dye X-3B over pillared bentonites containing iron, J. Hazard. Mater. 132 (2006) 196–201.
[32] C. Galindo, P. Jacques, A. Kalt, Photochemical and photocatalytic degradation of an indigoid dye: a case study of acid blue 74 (AB74), J. Photochem. Photobiol. A: Chem. 141 (2001) 47–56.
[33] C. Lizama, J. Freer, J. Baeza, H.D. Mansilla, Optimized photodegradation of Reactive Blue 19 on TiO_2 and ZnO suspensions, Catal. Today 76 (2002) 235–246.
[34] S. Sakthivel, B. Neppolian, M.V. Shankar, B. Arabindoo, M. Palanichamy, V. Murugesan, Solar photocatalytic degradation of azo dye: comparison of photocatalytic efficiency of ZnO and TiO_2, Solar Energy Mater. Solar Cells 77 (2003) 65–82.
[35] M.A. Behnajady, N. Modirshahla, R. Hamzavi, Kinetic study on photocatalytic degradation of C.I. Acid Yellow 23 by ZnO photocatalyst, J. Hazard. Mater. 133 (2006) 226–232.
[36] M.I. Stefan, A.R. Hoy, J.R. Bolton, Kinetics and mechanism of the degradation and mineralization of acetone in dilute aqueous solution sensitized by the UV photolysis of hydrogen peroxide, Environ. Sci. Technol. 30 (1996) 2382–2390.